Published in final edited form as:

J Leukoc Biol. 2022 December ; 112(6): 1543–1553. doi:10.1002/JLB.3MA0422-742R.

Contact-dependent, polarized acidification response during neutrophil–epithelial interactions

Ian M. Cartwright[1,2,3], **Alexander S. Dowdell**[1,2], **Camila Hanson**[1,2,3], **Rachael E. Kostelecky**[1,2], **Nichole Welch**[1,2], **Calen A. Steiner**[1,2], **Sean P. Colgan**[1,2,3]

[1]Mucosal Inflammation Program, University of Colorado Anschutz Medical Campus, Aurora, Colorado, USA

[2]Department of Medicine, University of Colorado Anschutz Medical Campus, Aurora, Colorado, USA

[3]Rocky Mountain Regional Veterans Affairs Medical Center, Aurora, Colorado, USA

Abstract

Neutrophil (PMN) infiltration during active inflammation imprints changes in the local tissue environment. Such responses are often accompanied by significant extracellular acidosis that result in predictable transcriptional responses. In this study, we explore the mechanisms involved in inflammatory acidification as a result of PMN–intestinal epithelial cell (IEC) interactions. Using recently developed tools, we revealed that PMN transepithelial migration (TEM)-associated inflammatory acidosis is dependent on the total number of PMNs present during TEM and is polarized toward the apical surface. Extending these studies, we demonstrate that physical separation of the PMNs and IECs prevented acidification, whereas inhibition of PMN TEM using neutralizing antibodies enhanced extracellular acidification. Utilizing pharmaceutical inhibitors, we demonstrate that the acidification response is independent of myeloperoxidase and dependent on reactive oxygen species generated during PMN TEM. In conclusion, inflammatory acidosis represents a polarized PMN–IEC-dependent response by an as yet to be fully determined mechanism.

Summary Sentence:

Inflammatory acidosis represents a polarized neutrophil–epithelial-dependent response independent of myeloperoxidase and ion efflux.

Keywords

inflammatory acidosis; myeloperoxidase; pH; transepithelial migration

Correspondence: Ian M. Cartwright, University of Colorado School of Medicine, 12700 East 19th Ave. MS B-146, Aurora, CO 80045, USA. Ian.Cartwright@CUAnschutz.edu.

AUTHORSHIP

I. M. C. and S. P. C. designed the research; I. M. C., C. H., and R. E. K. performed the research; I. M. C. analyzed the data; R. E. K., C. A. S., and N. W. provided reagents and technical support; I. M. C. and S. P. C. wrote the paper.

DISCLOSURE

The authors have stated explicitly that there are no conflicts of interest in connection with this article.

1 | INTRODUCTION

A key feature of many mucosal inflammatory diseases is the transepithelial migration (TEM) of neutrophils (PMNs) to sites of injury. TEM is a highly organized, multistep event with each step governed by distinct mechanisms. PMN TEM is initiated by PMN adhesion to the basolateral epithelial membrane in a leukocyte β_2 integrin CD11b/CD18-dependent manner and progresses through CD47-dependent mechanisms at the apical epithelial membrane.[1,2] Once PMN TEM has concluded, PMNs interact with intestinal epithelial cells (IECs) through CD55-dependent mechanisms that significantly impact inflammatory responses and wound healing.[3–5] In addition to direct interactions with IECs, it has recently been shown that PMN TEM plays a significant role in shaping the inflammatory microenvironment (e.g. inflammatory hypoxia and acidosis).[6,7] These observations suggest that PMN–IEC interactions are essential for modulating and regulating inflammation.

An often-underappreciated aspect of the inflammatory microenvironment is extracellular acidification. During active inflammation, extracellular pH can fall to as low as 3 (e.g., rheumatoid arthritis, cancer, and inflammatory bowel disease).[8–11] It is thought that the primary mechanism of tissue acidification is increased accumulation of lactic acid at sites of inflammation as a result of the infiltration and activation of inflammatory cells.[12] Tissue lactate levels can exceed 10 mM in rheumatic synovial fluid and within cancerous tissue, lactic acid levels can reach 40 mM.[8] However, it has been recently reported that PMN TEM-induced acidification occurs rapidly and that lactate levels measured during PMN TEM account for only a portion of the pH changes observed in inflammatory acidification.[6] This observation suggests an additional mechanism outside of lactic acid for inflammatory acidification.

In the present work, we sought to define the mechanisms of inflammatory acidification observed during active PMN TEM. We expanded on earlier observations of PMN TEM-induced acidification to show a polarized, PMN concentration-dependent acidification. Extracellular acidification was completely blocked when PMNs and IECs were physically separated. However, when TEM was inhibited using neutralizing antibodies directed against CD11b/18, CD47, or CD55, the acidification response was enhanced. Extending these studies, we demonstrate that the acidification response is independent of ion efflux and myeloperoxidase (MPO), but the use of multiple antioxidants significantly attenuated extracellular acidification following activated PMN–IEC interactions.

2 | MATERIALS AND METHODS

2.1 | PMN isolation and stimulation

Human PMNs were isolated from whole venous blood of healthy volunteers as described in detail previously[13] (IRB# 06–0853). Briefly, whole venous blood was collected in syringes containing anticoagulant (K_2EDTA at 1.8 mg/ml blood). Blood was gently layered over double-density Histopaque gradients (1119/1077) and centrifuged at 700×*g* in a swinging bucket rotor centrifuge for 30 min without brake. The resulting granulocyte layer was collected and residual RBCs lysed. PMNs were washed with ice-cold HBSS- (w/out $CaCl_2$ or $MgCl_2$), counted and used within 2 h of isolation.

2.2 | Cell culture

T84 (#CCL-248) and Caco2 (#HTB-37) human epithelial cell lines were obtained from American Type Culture Collection (ATCC) (Manassas, VA) and were cultured in 95% air with 5% CO_2 at 37°C according to instructions provided by ATCC. Where indicated, cells were cultured on 5.0 μM or 0.4 μm pore polyester transwell inserts for 10–14 days to obtain confluent cell monolayers as measured by transepithelial resistance (CoStar, Cambridge, MA). Bumetanide (10 μM), S3226 (5 μM), indole (1 mM), myricetin (10 μM), and 4-aminobenzoic hydrazide (4-ABAH) (500 μM) obtained from Sigma–Aldrich (St. Louis, MA) were added to sterile filtered HBSS (indole and 4-ABAH) or DMSO (bumetanide and S3226). Anti-CD11b (M1/70) and IgG1 rat isotype control monoclonal antibodies (10 μg/ml) were obtained from BioLegend (San Diego, CA). Anti-CD47 (B6H12) and IgG1 mouse isotype control monoclonal antibody (10 μg/ml) was obtained from Fisher Scientific (Hampton, NH). Anti-CD55 (clone OE-1) mouse monoclonal antibody (10 μg/ml) was produced as previously described.[14] All inhibitors were used at established, noncytotoxic concentrations.

2.3 | Measurement of extracellular pH

To measure real-time changes in extracellular pH, HydroDish HD24 (PreSens Precision Sensing, Regensburg, Germany) and a SDR Sensor-Dish Reader (PreSens Precision Sensing) were utilized. Briefly, T84 or Caco2 IECs were grown to confluence on the underside of Transwell 5.0 or 0.4 μm pore permeable supports as inserts or grown on the top-side of the permeable support as an insert. The inserts were placed into HBSS with $HCO3^-$ and without HEPES. 1 μM fMLP was added to the apical (bottom) chamber immediately prior to the addition of 1.5×10^6 PMNs to the basolateral side (top) and the pH was monitored every minute for 90 min at 37°C under atmospheric CO_2 levels. For each experiment, we averaged the data collected from 4 technical replicates.

2.4 | In vitro MPO assay

Following 90 min, permeable supports were removed from the HydroDish HD24 and 100 μl of 10% Triton X-100 was added to each well and incubated for 15 min at 4°C. Fifty microliters of 1 M citrate buffer, pH 4.2, was added to each well and gently swirled. Hundred microliters of the lysate was combined with a 100 mM citrate buffer containing 550 μg/ml ABTS diammonium salt (Sigma–Aldrich) and 6 mM H_2O_2 (Sigma–Aldrich). Reactions were incubated for 10 min at room temperature and the oxidation of ABTS measured by absorbance at 405 nm.

3 | RESULTS

3.1 | PMN TEM-associated extracellular acidification

Inflamed tissue has been associated with marked increase in tissue acidification and it has been recently shown that PMNs can promote extracellular acidification during TEM.[6,15,16] To better understand the potential mechanisms involved in PMN TEM-associated acidification, we used a model we developed to monitor extracellular pH in real-time during PMN TEM using varying number of PMNs (Figure 1(A)).[6] A chemotactic

agent (1 μM fMLP) was applied to the apical surface and 5×10^5 to 2×10^6 PMNs were applied to the basolateral surface to allow for transmigration in the physiologically relevant basolateralto-apical direction. As shown in Figure 1(B), there is a significant dose-dependent acidification response to PMNs ($p < 0.0001$). The change in extracellular pH following the transmigration of 5×10^5 PMNs, −0.54 ± 0.03, was significantly less than the −0.90 ± 0.03 and −1.25 ± 0.02 observed with 1×10^6 and 2×10^6 PMNs, respectively (Figure 1(C), $p < 0.0001$ for both). To determine if different starting amounts of PMNs resulted in changes in total PMN TEM, we quantified PMN TEM by analyzing the bottom chamber (apical surface) of the transwell for MPO activity, as previously descripted,[17] 90 min after the start of PMN TEM. As shown in Figure 1(D), there is a significant decrease in MPO activity as the number of starting PMN decreases (3.69 ± 0.09, 1.59 ± 0.05, and 0.70 ± 0.02 OD405 for 2×10^6, 1×10^6, and 5×10^5 PMNs, respectively, $p < 0.0001$ for all comparisons). We extended these studies to include an additional IEC line Caco-2, clone C2BBe1.[18] As shown in Figures 1(E) and 1(F), following PMN TEM in the Caco-2 cell line, there is a significant decrease in extracellular pH in the presence of transmigration when compared with Caco-2 inserts with no PMN TEM (−2.21 ± 0.1 and −1.70 ± 0.07, $p < 0.02$). Interestingly, there is a significant difference in extracellular pH between the T84 and Caco2 controls. However, when compared the change in pH between the controls and activated PMN inverts, there is no significant difference (−0.96 ± 0.2 and −0.55 ± 0.1, for T84 and Caco2, respectively, p = not significant). PMN TEM was confirmed by assaying MPO activity. There was no significant difference in PMN TEM when comparing T84 and Caco-2 IECs (Figure 1(G), p = not significant). In summary, these data reveal that PMN TEM-induced extracellular acidification is dose and time dependent.

3.2 | Polarized acidification response to PMN TEM

Within the gastrointestinal tract, IECs exist as a highly organized and polarized monolayer with distinct apical and basolateral surfaces.[19] It has been observed that PMNs can interact with epithelial cells at both the apical and basolateral surfaces through different mechanism.[20,21] To examine the acidification response to apical IECs and PMNs interactions, T84 IECs were plated as inserts, as shown in Figure 2(A), and 1.5×10^6 PMNs were applied to the apical surface and allowed to transmigrate in the apical to basolateral direction for 90 min. As show in Figures 2(B) and 2(C), significant extracellular acidification was only observed when activated PMN interacted with the basolateral surface and migrated in the basolateral to apical direction. Basolateral to apical transmigration resulted in a −1.38 ± 0.2 pH change as compared with apical to basolateral transmigration, which had a pH change of −0.15 ± 0.03 ($p < 0.0001$). There was no significant difference in the pH change when comparing nonactivated and activated PMNs at the apical surface (−0.13 ± 0.2 and −0.15 ± 0.03, respectively, p = not significant). We next examined if the lack of extracellular acidification was due to the PMNs not transmigrating in the apical to basolateral direction. As shown in Figure 2(D), there was significant PMN TEM in the apical to basolateral (inserts) direction when compared with nonactivated PMN inserts (1.44 ± 0.1 and 0.22 ± 0.01 OD405, respectively, $p < 0.005$). There was significantly less PMN TEM across the inserts when compared with inverts (1.44 ± 0.1 and 2.31 ± 0.3 OD 405, respectively, $p < 0.01$).

3.3 | PMN–epithelial cell interaction is required for inflammatory acidification

Furthering these studies, we examined the need for PMN–IEC interaction in inflammatory acidification. PMN TEM was inhibited through the use of small pore inserts and neutralizing antibodies. As shown in Figures 3(A) and 3(B), 0.4 μm permeable supports were used to physically separate PMNs from IECs and prevent PMN TEM. When using a 0.4 μm permeable support, there was no increase in MPO activity between the nonactivated PMN and activated PMN (Figure 3(B), p = not significant). As previously shown,[6] when PMNs and IECs were physically separated there was significantly less change in extracellular pH when compared with IEC and activated PMN on 5.0 μm permeable supports (−0.19 ± 0.2 and −1.08 ± 0.07 change in pH, $p < 0.01$) (Figures 3(C) and 3(D)). We next utilized functionally inhibitory anti-CD11b, anti-CD47, and anti-CD55 antibodies to inhibit PMN TEM at both the basolateral surface (CD11b and CD47) and at the apical surface (CD55) (Figure 4(B), see insert).[22–24] Both anti-CD47 and anti-CD11b significantly inhibited PMN TEM when compared with IgG controls, as determined by MPO activity (Figure 4(A), $p < 0.0001$). Interestingly, when PMN TEM was blocked using antibodies, extracellular acidification responses were maintained in the presence of activated PMN (−1.94 ± 0.1 and −1.63 ± 0.1 change in pH for anti-CD47 and CD11b, respectively) (Figures 4(B) and 4(C)). When compared with IgG controls, the change in pH observed in anti-CD47 and CD11b treated inverts was significantly larger ($p < 0.001$) (Figures 4(B) and 4(C)). To examine if PMN retention at the apical surface post-TEM influenced acidification, CD55 was blocked using a functionally inhibitory anti-CD55 antibody.[14] When CD55 is blocked with the use of a functionally inhibitory antibody, PMN TEM is partially inhibited and PMNs accumulate at the apical surface.[14] As shown in Figures 4(A)–4(C), anti-CD55 partially inhibited PMN TEM, but did not significantly change extracellular acidification when compared to anti-CD47 and CD11b treated inverts (−2.05 ± 0.2, 1.94 ± 0.1, and −1.63 ± 0.1 change in pH for anti-CD55, CD47, and CD11b, respectively (p = not significant). We extended these studies to examine if antibody ligation activates PMNs and produces a factor that impacts acidification in the absence of TEM. T84 IECs were grown to confluency as inverts on 0.4 μm permeable supports. When IECs were physically separated from PMNs, there was no significant extracellular acidification in the presence of anti-CD47/11b both in the presence and absence of fMLP (Figure 4(D)). In summary, it is shown that inflammatory acidification is independent of PMN TEM but requires PMNs and IECs interaction.

3.4 | Inflammatory acidification is independent of ion transport

To better understand the potential mechanism involved in inflammatory acidification, we examined the impact of Cl^- and H^+ secretion on extracellular acidification during PMN TEM. Apical Cl^- secretion was blocked by inhibiting the basolateral $Na^+K^+2Cl^-$ cotransporter using a well-established nontoxic dose of 10 μM bumetanide.[25–27] As shown in Figure 5(A), there was significant PMN-induced acidification in IECs pretreated with 10 μM bumetanide when compared with bumetanide-treated IECs exposed to nonactivated PMNs (−1.31 ± 0.1 and −0.40 ± 0.2 change in pH respectively, $p < 0.01$). The prominent IEC apical hydrogen transporter, NHE3, was inhibited using 5 μM S3226, a potenant and selective inhibitor of NHE3.[28,29] Inhibition of apical H^+ by S3226 had no significant impact on extracellular acidification when compared with vehicle controls (−0.95 ± 0.2 and −1.27

± 0.2, respectively, p = not significant). These observations indicate that inflammatory acidification is not the result of ion efflux from the IEC during PMN TEM.

3.5 | Inflammatory acidosis is inhibited by indole but independent of MPO

We extended our studies to examine the role of MPO in inflammatory acidification. PMN MPO was inhibited using the potent and selective MPO inhibitor, 4-ABAH, and the microbial-derived metabolite indole.[17,30] As shown in Figure 6(A), there was no significant difference in extracellular pH when comparing PMNs transmigrated in the presence of 4-ABAH (−1.20 ± 0.2) and absence (−1.29 ± 0.1) (p = not significant). Interestingly, the presence of indole significant attenuated extracellular acidification when compared with vehicle controls (−0.72 ± 0.05 and −1.29 ± 0.1 respectively, $p < 0.01$). Furthermore, there was no significant difference in extracellular acidification when compared activated and nonactivated PMN in the presence of indole (−0.72 ± 0.05 and −0.36 ± 0.1 respectively, p = not significant). In order to examine the influence of 4-ABAH and indole on total PMN TEM, we collected the media from the large chamber and counted the number of transmigrated PMNs. As shown in Figure 6(B), fewer PMNs transmigrated in the presence of indole as compared with vehicle control and 4-ABAH-treated inserts ($4.44 \times 10^5 \pm 5.2 \times 10^4$, $1.06 \times 10^6 \pm 10^5$, and $9.02 \times 10^5 \pm 4.0 \times 10^4$ PMNs, respectively, $p < 0.05$). In addition to being a MPO inhibitor, indole has also been shown to be an antioxidant.[31] To further examine if inflammatory acidification could be inhibited by antioxidants, we utilized DMSO and myricetin, both well-defined reactive oxygen species scavenger.[32–36] As shown in Figures 6(C) and 6(D), 1% DMSO and 10 μM myricetin significantly reduced extracellular acidification when compared with vehicle controls (−0.72 ± 0.08, −0.57 ± 0.1, and −1.33 ± 0.04 change in pH respectively, $p < 0.001$). Furthermore, treatment with 1% DMSO did not affect PMN TEM when compared with vehicle controls (Figure 6(D), p = not significant). Similar to that of indole, treatment with 10 μM myricetin significantly inhibited PMN TEM when compared with vehicle controls (Figure 6(D), $p < 0.005$). In conclusion, these observations indicate that inflammatory acidification is not a result of MPO activity and can be attenuated using antioxidants.

4 | DISCUSSION

An understanding of how inflamed tissues become acidic is a relatively understudied area. Specifically, the mechanisms involved in acidification during PMN–IEC interaction remain unclear. In active ulcerative colitis, tissue pH in the colon of individuals with active disease can fall to as low as a pH 5, where healthy individuals maintain colonic pH in the range of 6.8–7.4.[9,12,37] This acidification is often attributed to increased accumulation of lactic acid resulting from enhanced glycolysis during active inflammation.[8] However, in a recent study, we demonstrated that the decrease in pH observed during PMN TEM was much larger than what was predicted based on observed lactic acid concentrations. Furthermore, measurable lactic acid concentrations took several hours to increase, whereas the most significant PMN TEM-induced acidification occurred within the first 90 min. These results have revealed that lactic acid is not solely responsible for inflammatory acidification and is supported by reports which suggest lactic acid only accounts for 30–60% of acidification observed

in tumors.[38–40] The present study provides significant new insight into the acidification response to PMN–IEC interaction.

Initially, we investigated the impact of total number of transmigrated PMN on extracellular acidification. We revealed that as the total number of PMN increases, the greater the change in extracellular pH following TEM. Extending these experiments, we determined that the acidification response to PMN–IEC interaction was a polarized, with acidification only observed on the apical surface. This observation is consistent with the findings that inflammation in both the colon and in the lungs is associated with luminal acidification.[10,41,42]

We extended our studies to further examine the role of TEM in extracellular acidification. We confirmed our prior observation the inhibiting PMN TEM through physical separation of PMNs and IECs prevented extracellular acidification.[6] We expanded upon this observation and blocked PMN TEM using neutralizing antibodies. During TEM, PMNs interact with the IECs at multiple points through a wide range of adhesion molecules.[43] PMN CD11b/18 is required for adhesion to the IEC basolateral surface, though the exact mechanism remains unclear.[44,45] CD47 is expressed on both the IECs and PMNs, blocking antibodies targeting CD47 inhibits PMN TEM, but does not inhibit basolateral adhesion of PMNs to IECs.[2] CD55, also referred to as decay acceleration factor, is a glycosyl-phosphatidyinositoal-linked protein located on the apical surface of IECs. CD55 serves as an antiadhesive surface protein that regulates the rate of PMNs migration, blocking antibodies targeting CD55 results in the accumulation of PMNs at the IECs apical surface.[14] Surprisingly, we observed significant acidification when PMN TEM was inhibited using antibodies targeting either CD11b,CD47, or CD55. Unlike the 0.4 μm pore permeable supports, PMN–IEC cocultures treated with anti-CD11b, CD47, or CD55 are still able to interact with the IECs through the larger 5.0 μm pores, suggesting that physically contact between PMN and IEC is required for the extracellular acidification response. The requirement for PMN and IEC interaction, not a soluble factor, in extracellular acidification is supported by the observation that there is no extracellular acidification when IEC grown on 0.4 μm pore permeable supports in the presence of anti-CD11b/CD47/CD55.

Considering PMN TEM induces Cl^- section,[46] via the apical cystic fibrosis transmembrane conductance regulator (CFTR), that is followed by the activation Na^+/H^+ exchanger isoform 3 (NHE3),[47] we defined the influence of ion efflux on extracellular acidification. To inhibit apical chloride secretion, bumetanide was utilized to inhibit the NaK_2Cl cotransporter, with resultant inhibition of efflux through the apical Cl^- CFTR. It is notable that in cystic fibrosis patients, who lack a functional CFTR, there is a marked decrease in lung mucosal pH.[48,49] Additionally, it has been shown that the NHE3 transporter plays a significant role in sodium bicarbonate secretion and the regulation of intracellular pH.[50,51] The potent and selective NHE3 inhibitor S3226 was used to inhibit NHE3, which decreases apical secretion of H^+.[29] When apical Cl^- or H^+ efflux was inhibited, we observed no change in PMN–IEC interaction induced extracellular acidification.

Upon activation, PMNs undergo a NADPH oxidase burst, consuming a large amount of O_2 and generating superoxide radicals.[52] These superoxide radicals are metabolized

by superoxide dismutase into O_2 and hydrogen peroxide. The PMN then utilizes MPO to convert hydrogen peroxide to hypochlorous acid.[53] Based on the ability of PMN to generate hypochlorous acid through MPO, we investigated the impact of MPO on extracellular acidification. This analysis revealed that the potent MPO inhibitor, 4-ABAH, had no influence on extracellular acidification, whereas indole, a potent MPO inhibitor,[17] significantly inhibited extracellular acidification following PMN–IEC interactions. In addition to its role as an MPO inhibitor,[17] indole is also a potent antioxidant.[54] Within PMN hydroxyl radicals are also generated from the reaction of hydrogen peroxide and superoxide with Fe^{3+}.[55] To examine the significance of hydroxyl radicals in extracellular acidification, we examined changes in extracellular pH in the presence of the antioxidants DMSO and myricetin. DMSO is a hydroxyl radical scavenger and has been used in the radiation biology field as a radioprotectant because of this property.[32,34,56] Myricetin is a flavonoid with potentant antioxidant properties and considered to be an excellent scavenger of intracellular reactive oxygen species.[57,58] Studies have shown that oxidative stress, including increased accumulation of superoxide and hydroxyl radicals, induces cytosolic acidification in a wide range of tissue types.[59–61] In the presence of 1% DMSO or 10 μM myricetin, we observed a significant attenuation in extracellular acidification, similar to that observed with indole. These results suggest that the extracellular acidification occurring during PMN–IEC interactions is a result of free radicals produced during the PMN oxidative burst.

Taken together, these results provide new insight into the role of PMN–IEC interaction in inflammatory acidification. Our results highlight a polarized, IEC-dependent, and TEM-independent acidification response to PMNs. Activated PMNs interact with IECs to drive an apical acidification response that does not require TEM or PMN MPO activity. Such findings could implicate an adaptive mechanism to mold the luminal microbiota. Studies in other organs, such as the kidney, have revealed that metabolic acidosis induces antimicrobial peptides that have the potential to promote protection from pyelonephritis.[62] Whether such mechanisms are at ply in the intestine awaits further investigation. In conclusion, while we do not know the exact mechanism(s) of polarized acidification, the present observations implicate free radicals, produced during the PMN oxidative burst, as a driver of extracellular acidification.

ACKNOWLEDGMENTS

This work was supported by NIH grants DK050189 and DK095491 and by the Veterans Administration Awards BX002182 and BX005710.

Abbreviations:

IEC	intestinal epithelial cell
MPO	myeloperoxidase
PMN	polymorphonuclear leukocyte, neutrophil
TEM	transepithelial migration

REFERENCES

1. Zen K, Babbin BA, Liu Y, Whelan JB, Nusrat A, Parkos CA. JAM-C is a component of desmosomes and a ligand for CD11b/CD18-mediated neutrophil transepithelial migration. Mol Biol Cell. 2004;15:3926–37. [PubMed: 15194813]
2. Parkos CA, Colgan SP, Liang TW, et al. CD47 mediates post-adhesive events required for neutrophil migration across polarized intestinal epithelia. J Cell Biol. 1996;132:437–50. [PubMed: 8636220]
3. Sumagin R, Brazil JC, Nava P, et al. Neutrophil interactions with epithelial-expressed ICAM-1 enhances intestinal mucosal wound healing. Mucosal Immunol. 2016;9:1151–62. [PubMed: 26732677]
4. Nava P, Koch S, Laukoetter MG, et al. Interferon-gamma regulates intestinal epithelial homeostasis through converging beta-catenin signaling pathways. Immunity. 2010;32:392–402. [PubMed: 20303298]
5. Nava P, Capaldo CT, Koch S, et al. JAM-A regulates epithelial proliferation through Akt/beta-catenin signalling. EMBO Rep. 2011;12:314–20. [PubMed: 21372850]
6. Cartwright IM, Curtis VF, Lanis JM, et al. Adaptation to inflammatory acidity through neutrophil-derived adenosine regulation of SLC26A3. Mucosal Immunol. 2020;13:230–244. [PubMed: 31792360]
7. Campbell EL, Bruyninckx WJ, Kelly CJ, et al. Transmigrating neutrophils shape the mucosal microenvironment through localized oxygen depletion to influence resolution of inflammation. Immunity. 2014;40:66–77. [PubMed: 24412613]
8. Pucino V, Bombardieri M, Pitzalis C, Mauro C. Lactate at the crossroads of metabolism, inflammation, and autoimmunity. Eur J Immunol. 2017;47:14–21. [PubMed: 27883186]
9. Roediger WE, Lawson MJ, Kwok V, Grant AK, Pannall PR. Colonic bicarbonate output as a test of disease activity in ulcerative colitis. J Clin Pathol. 1984;37:704–7. [PubMed: 6327778]
10. Nugent SG, Kumar D, Rampton DS, Evans DF. Intestinal luminal pH in inflammatory bowel disease: possible determinants and implications for therapy with aminosalicylates and other drugs. Gut. 2001;48:571–7. [PubMed: 11247905]
11. Fallingborg J, Christensen LA, Jacobsen BA, Rasmussen SN. Very low intraluminal colonic pH in patients with active ulcerative colitis. Dig Dis Sci. 1993;38:1989–93. [PubMed: 8223071]
12. Rajamaki K, Nordstrom T, Nurmi K, et al. Extracellular acidosis is a novel danger signal alerting innate immunity via the NLRP3 inflamma-some. J Biol Chem. 2013;288:13410–9. [PubMed: 23530046]
13. Campbell EL, Louis NA, Tomassetti SE, et al. Resolvin E1 promotes mucosal surface clearance of neutrophils: a new paradigm for inflammatory resolution. FASEB J. 2007;21:3162–70. [PubMed: 17496159]
14. Lawrence DW, Bruyninckx WJ, Louis NA, et al. Antiadhesive role of apical decay-accelerating factor (CD55) in human neutrophil transmigration across mucosal epithelia. J Exp Med. 2003;198:999–1010. [PubMed: 14530374]
15. Wike-Hooley JL, Haveman J, Reinhold HS. The relevance of tumour pH to the treatment of malignant disease. Radiother Oncol. 1984;2:343–66. [PubMed: 6097949]
16. Fiddian-Green RG. Gastric intramucosal pH, tissue oxygenation and acid-base balance. Br J Anaesth. 1995;74:591–606. [PubMed: 7772437]
17. Alexeev EE, Dowdell AS, Henen MA, et al. Microbial-derived indoles inhibit neutrophil myeloperoxidase to diminish bystander tissue damage. FASEB J. 2021;35:e21552. [PubMed: 33826788]
18. Peterson MD, Mooseker MS. Characterization of the enterocyte-like brush border cytoskeleton of the C2BBe clones of the human intestinal cell line, Caco-2. J Cell Sci. 1992;102:581–600. [PubMed: 1506435]
19. Massey-Harroche D. Epithelial cell polarity as reflected in enterocytes. Microsc Res Tech. 2000;49:353–62. [PubMed: 10820519]
20. Edens HA, Levi BP, Jaye DL, et al. Neutrophil transepithelial migration: evidence for sequential, contact-dependent signaling events and enhanced paracellular permeability independent of transjunctional migration. J Immunol. 2002;169:476–86. [PubMed: 12077279]

21. Reaves TA, Colgan SP, Selvaraj P, et al. Neutrophil transepithelial migration: regulation at the apical epithelial surface by Fc-mediated events. Am J Physiol Gastrointest Liver Physiol. 2001;280:G746–54. [PubMed: 11254502]
22. Liu Y, Merlin D, Burst SL, Pochet M, Madara JL, Parkos CA. The role of CD47 in neutrophil transmigration. Increased rate of migration correlates with increased cell surface expression of CD47. J Biol Chem. 2001;276:40156–66. [PubMed: 11479293]
23. Zen K, Liu Y, Cairo D, Parkos CA. CD11b/CD18-dependent interactions of neutrophils with intestinal epithelium are mediated by fucosylated proteoglycans. J Immunol. 2002;169:5270–8. [PubMed: 12391246]
24. Balsam LB, Liang TW, Parkos CA. Functional mapping of CD11b/CD18 epitopes important in neutrophil-epithelial interactions: a central role of the I domain. J Immunol. 1998;160:5058–65. [PubMed: 9590256]
25. McNamara B, Winter DC, Cuffe JE, O'Sullivan GC, Harvey BJ. Basolateral K+ channel involvement in forskolin-activated chloride secretion in human colon. J Physiol. 1999;519:251–60. [PubMed: 10432355]
26. Wallace DP, Grantham JJ, Sullivan LP. Chloride and fluid secretion by cultured human polycystic kidney cells. Kidney Int. 1996;50:1327–36. [PubMed: 8887295]
27. Keely S, Kelly CJ, Weissmueller T, et al. Activated fluid transport regulates bacterial-epithelial interactions and significantly shifts the murine colonic microbiome. Gut Microbes. 2012;3:250–60. [PubMed: 22614705]
28. Gleeson D. Acid-base transport systems in gastrointestinal epithelia. Gut. 1992;33:1134–45. [PubMed: 1398242]
29. Schwark JR, Jansen HW, Lang HJ, Krick W, Burckhardt G, Hropot M. S3226, a novel inhibitor of Na+/H+ exchanger subtype 3 in various cell types. Pflugers Arch. 1998;436:797–800. [PubMed: 9716715]
30. Kettle AJ, Gedye CA, Winterbourn CC. Mechanism of inactivation of myeloperoxidase by 4-aminobenzoic acid hydrazide. 1997;321:503–8.
31. Herraiz T, Galisteo J. Endogenous and dietary indoles: a class of antioxidants and radical scavengers in the ABTS assay. Free Radic Res. 2004;38:323–31. [PubMed: 15129740]
32. Tuncer S, Gurbanov R, Sheraj I, Solel E, Esenturk O, Banerjee S. Low dose dimethyl sulfoxide driven gross molecular changes have the potential to interfere with various cellular processes. Sci Rep. 2018;8:14828.
33. Shimizu S, Simon RP, Graham SH. Dimethylsulfoxide (DMSO) treatment reduces infarction volume after permanent focal cerebral ischemia in rats. Neurosci Lett. 1997;239:125–7. [PubMed: 9469672]
34. deLara CM, Jenner TJ, Townsend KM, Marsden SJ, O'Neill P. The effect of dimethyl sulfoxide on the induction of DNA double-strand breaks in V79–4 mammalian cells by alpha particles. Radiat Res. 1995;144:43–9. [PubMed: 7568770]
35. Wang ZH, Ah Kang K, Zhang R, et al. Myricetin suppresses oxidative stress-induced cell damage via both direct and indirect antioxidant action. Environ Toxicol Pharmacol. 2010;29:12–8. [PubMed: 21787576]
36. Ong KC, Khoo HE. Biological effects of myricetin. Gen Pharmacol. 1997;29:121–6. [PubMed: 9251891]
37. Lardner A. The effects of extracellular pH on immune function. J Leukoc Biol. 2001;69:522–30. [PubMed: 11310837]
38. Mookerjee SA, Goncalves RLS, Gerencser AA, Nicholls DG, Brand MD. The contributions of respiration and glycolysis to extracellular acid production. Biochim Biophys Acta. 2015;1847:171–181. [PubMed: 25449966]
39. Newell K, Franchi A, Pouyssegur J, Tannock I. Studies with glycolysis-deficient cells suggest that production of lactic acid is not the only cause of tumor acidity. Proc Natl Acad Sci USA. 1993;90:1127–31. [PubMed: 8430084]
40. Kato Y, Ozawa S, Miyamoto C, et al. Acidic extracellular microenvironment and cancer. Cancer Cell Int. 2013;13:89. [PubMed: 24004445]

41. Hunt JF, Fang K, Malik R, et al. Endogenous airway acidification. Implications for asthma pathophysiology. Am J Respir Crit Care Med. 2000;161:694–9. [PubMed: 10712309]
42. Fischer H, Widdicombe JH, Illek B. Acid secretion and proton conductance in human airway epithelium. Am J Physiol Cell Physiol. 2002;282:C736–43. [PubMed: 11880261]
43. Zemans RL, Colgan SP, Downey GP. Transepithelial migration of neutrophils: mechanisms and implications for acute lung injury. Am J Respir Cell Mol Biol. 2009;40:519–35. [PubMed: 18978300]
44. Zen K, Parkos CA. Leukocyte-epithelial interactions. Curr Opin Cell Biol. 2003;15:557–64. [PubMed: 14519390]
45. Parkos CA, Delp C, Arnaout MA, Madara JL. Neutrophil migration across a cultured intestinal epithelium. Dependence on a CD11b/CD18-mediated event and enhanced efficiency in physiological direction. J Clin Invest. 1991;88:1605–12. [PubMed: 1682344]
46. Nash S, Parkos C, Nusrat A, Delp C, Madara JL. In vitro model of intestinal crypt abscess. A novel neutrophil-derived secretagogue activity. J Clin Invest. 1991;87:1474–7. [PubMed: 2010557]
47. Engevik AC, Goldenring JR. Trafficking ion transporters to the apical membrane of polarized intestinal enterocytes. Cold Spring Harb Perspect Biol. 2018;10.
48. Tang XX, Ostedgaard LS, Hoegger MJ, et al. Acidic pH increases airway surface liquid viscosity in cystic fibrosis. J Clin Invest. 2016;126:879–91. [PubMed: 26808501]
49. Poschet J, Perkett E, Deretic V. Hyperacidification in cystic fibrosis: links with lung disease and new prospects for treatment. Trends Mol Med. 2002;8:512–9. [PubMed: 12421684]
50. Furukawa O, Bi LC, Guth PH, Engel E, Hirokawa M, Kaunitz JD. NHE3 inhibition activates duodenal bicarbonate secretion in the rat. Am J Physiol Gastrointest Liver Physiol. 2004;286:G102–9. [PubMed: 12881227]
51. Yeung CH, Breton S, Setiawan I, Xu Y, Lang F, Cooper TG. Increased luminal pH in the epididymis of infertile c-ros knockout mice and the expression of sodium-hydrogen exchangers and vacuolar proton pump H+-ATPase. Mol Reprod Dev. 2004;68:159–68. [PubMed: 15095336]
52. Henderson LM, Chappell JB, Jones OT. The superoxide-generating NADPH oxidase of human neutrophils is electrogenic and associated with an H+ channel. Biochem J. 1987;246:325–9. [PubMed: 2825632]
53. Nguyen GT, Green ER, Mecsas J. Neutrophils to the ROScue: mechanisms of NADPH oxidase activation and bacterial resistance. Front Cell Infect Microbiol. 2017;7:373. [PubMed: 28890882]
54. Kumar D, Sharma S, Kalra S, Singh G, Monga V, Kumar B. Medicinal perspective of indole derivatives: recent developments and structure-activity relationship studies. Curr Drug Targets. 2020;21:864–891. [PubMed: 32156235]
55. Winterbourn CC. Myeloperoxidase as an effective inhibitor of hydroxyl radical production. Implications for the oxidative reactions of neutrophils. J Clin Invest. 1986;78:545–50. [PubMed: 3016031]
56. Ewing D. The effects of dimethylsulfoxide (DMSO) on the radiation sensitivity of bacterial spores. Radiat Res. 1982;90:348–55. [PubMed: 6805035]
57. Gordon MH, Roedig-Penman A. Antioxidant activity of quercetin and myricetin in liposomes. Chem Phys Lipids. 1998;97:79–85. [PubMed: 10081150]
58. Barzegar A. Antioxidant activity of polyphenolic myricetin in vitro cell-free and cell-based systems. Mol Biol Res Commun. 2016;5:87–95. [PubMed: 28097162]
59. Singh Y, Zhou Y, Zhang S, et al. Enhanced reactive oxygen species production, acidic cytosolic pH and upregulated Na+/H+ exchanger (NHE) in dicer deficient CD4+ T Cells. Cell Physiol Biochem. 2017;42:1377–1389. [PubMed: 28704808]
60. Majdi A, Mahmoudi J, Sadigh-Eteghad S, Golzari SE, Sabermarouf B, Reyhani-Rad S. Permissive role of cytosolic pH acidification in neurodegeneration: a closer look at its causes and consequences. J Neurosci Res. 2016;94:879–87. [PubMed: 27282491]
61. Mulkey DK, Henderson RA 3rd, Ritucci NA, Putnam RW, Dean JB. Oxidative stress decreases pHi and Na(+)/H(+) exchange and increases excitability of solitary complex neurons from rat brain slices. Am J Physiol Cell Physiol. 2004;286:C940–51. [PubMed: 14668260]

62. Peng H, Purkerson JM, Freeman RS, Schwaderer AL, Schwartz GJ. Acidosis induces antimicrobial peptide expression and resistance to uropathogenic E. coli infection in kidney collecting duct cells via HIF-1alpha. Am J Physiol Renal Physiol. 2020;318:F468–F474. [PubMed: 31841391]

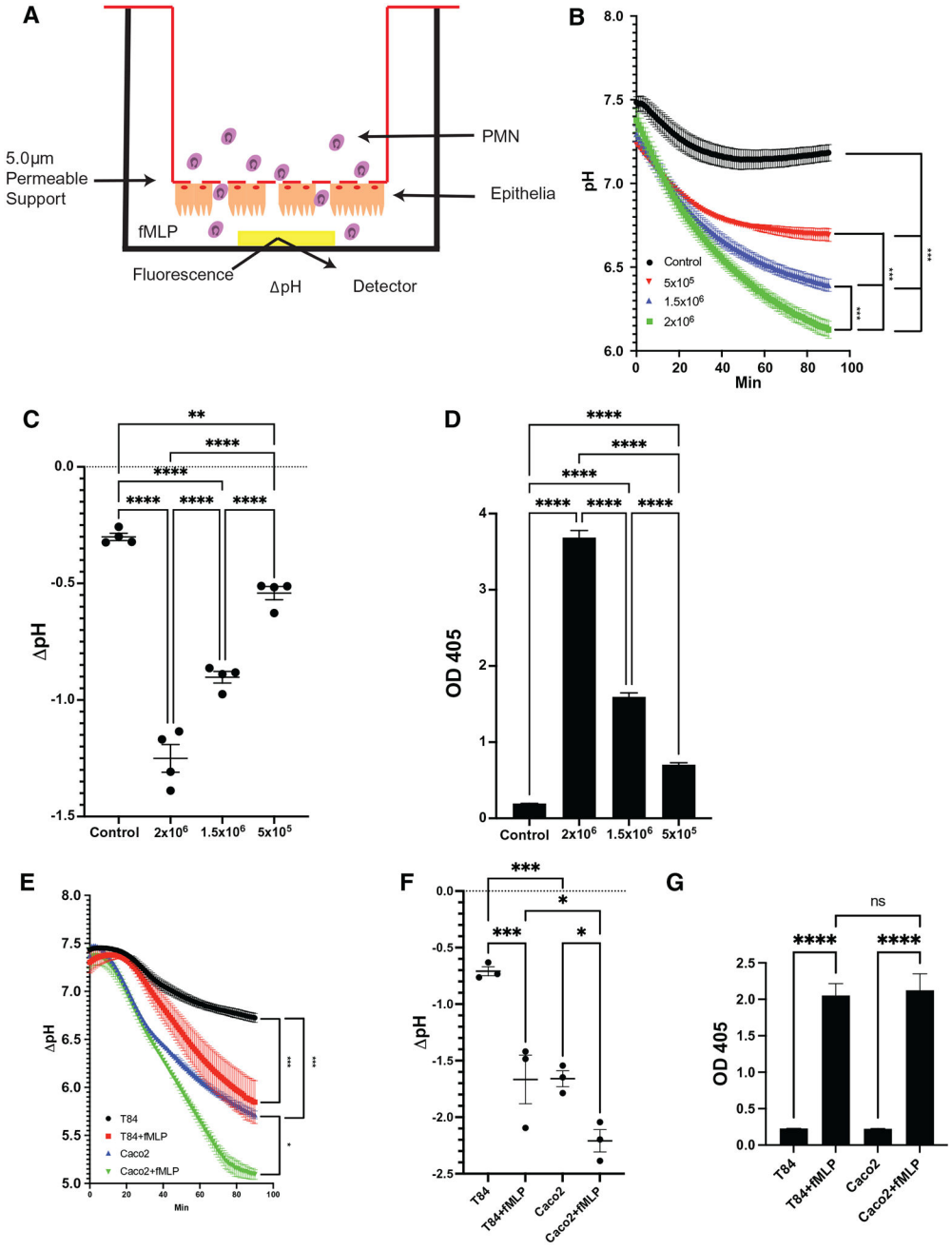

FIGURE 1.

PMN induced acidification. (A) Model of extracellular pH monitoring assay for basolateral to apical transmigration. (B) Changes in extracellular pH. 2×10^6, 1.5×10^6, and 5×10^5 PMNs were transmigrated across confluent T84 monolayers and the extracellular pH was recorded every minute for 90 min. The control is 2×10^6 PMNs added to the top apical chamber in the absence of fMLP. Data are expressed as pH ($n = 4$). (C) At T90, the difference between starting and ending pH were calculated. Data are expressed as change in pH. (D) Quantification of MPO activity at T90 ($n = 4$). (E) Changes in extracellular pH. 1.5×10^6 PMNs were transmigrated across confluent T84 or Caco2 monolayers and the

extracellular pH was recorded every minute for 90 min. In the controls (T84 and Caco2), 1.5 × 10^6 PMNs were added to the apical chamber in the absence of fMLP. Data are expressed as pH ($n = 4$). (F) At T90, the difference between starting and ending pH were calculated. Data are expressed as change in pH. (G) Quantification of MPO activity at T90 ($n = 4$). *N* = number of independent experiments performed, separate passages of cells were used for each experiment. The data for each experiment were pooled and expressed as the mean ± SEM and *p* value determined by ANOVA. $^{**}p < 0.01$, $^{***}p < 0.001$, $^{****}p < 0.0001$

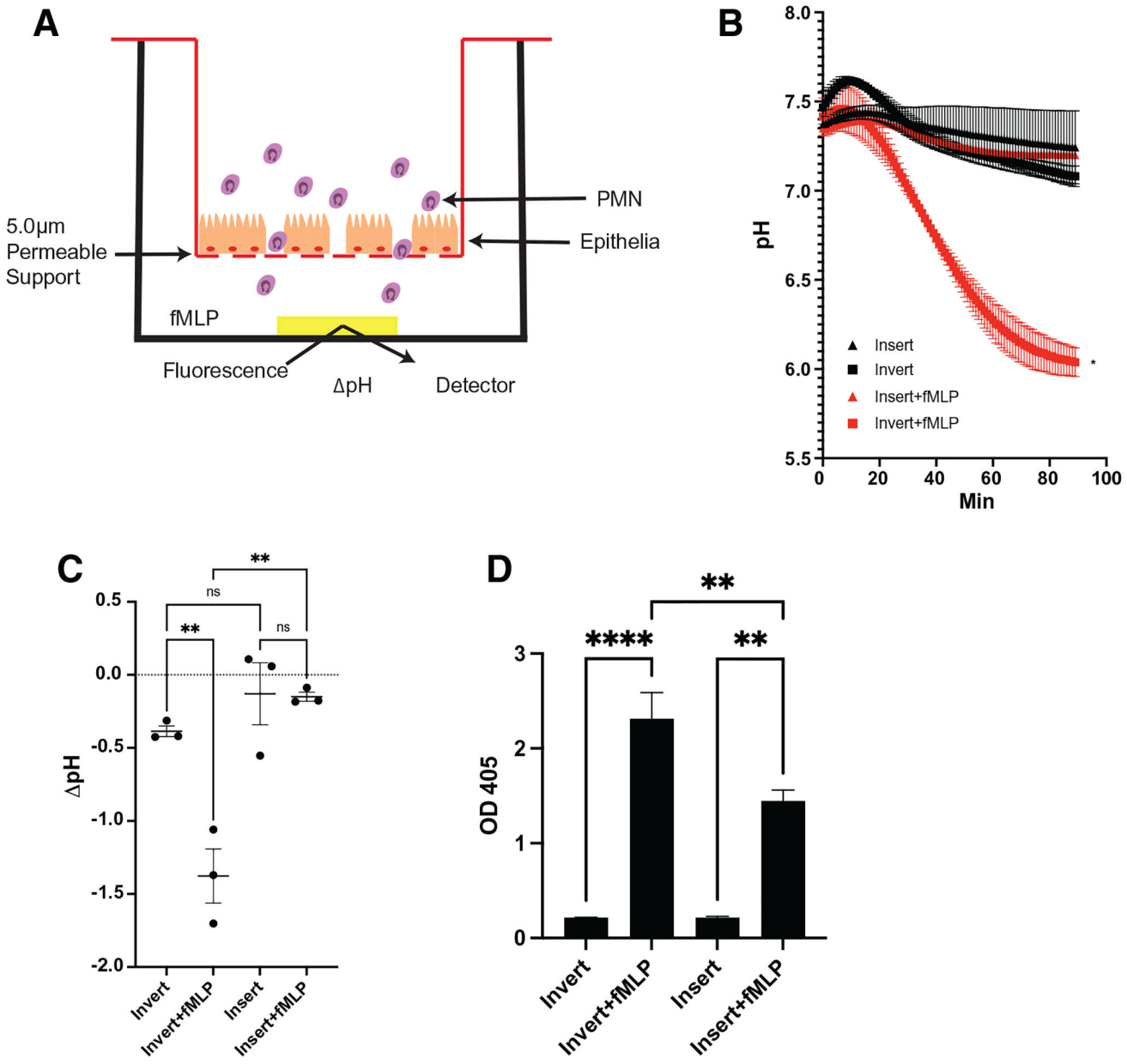

FIGURE 2.

Polarized acidification during PMN TEM. (A) Model of extracellular pH monitoring assay for apical to basolateral transmigration. (B) Changes in extracellular pH. 1.5×10^6 PMNs were transmigrated apical to basolateral (insert) or basolateral to apical (invert) across confluent T84 monolayers and the extracellular pH was recorded every minute for 90 min. In the controls (invert and insert), 1.5×10^6 PMNs were added in the absence of fMLP. Data are expressed as pH ($n = 3$). (C) At T90, the difference between starting and ending pH were calculated. Data are expressed as change in pH. (D) Quantification of MPO activity at T90 ($n = 3$). N = number of independent experiments performed, separate passages of cells were used for each experiment. The data for each experiment were pooled and expressed as

the mean ± SEM and p value determined by ANOVA. **$p < 0.01$, ***$p < 0.001$, ****$p < 0.0001$

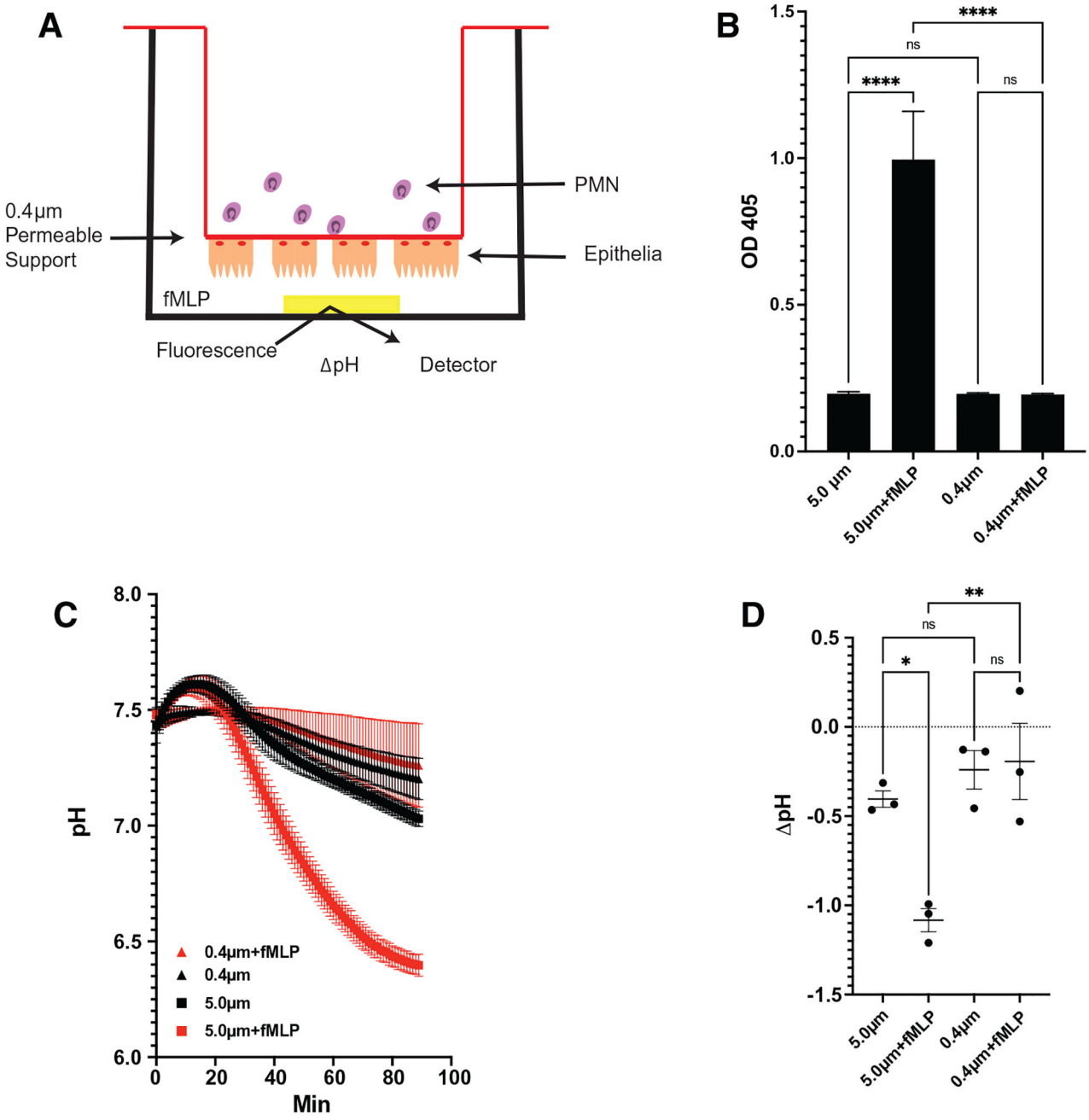

FIGURE 3.

Role of PMN/epithelial cell interaction in PMN-associated acidification. (A) Model of extracellular pH monitoring assay using small pore (0.4 μm) permeable supports. (B) Quantification of MPO activity at T90 (n = 3). (C) Changes in extracellular pH. 1.5 × 10^6 PMNs were transmigrated apical to basolateral across confluent T84 monolayers grown on 0.4 or 5.0 μm permeable supports and the extracellular pH was recorded every minute for 90 min. In the controls (0.4 and 5.0 μm), 1.5 × 10^6 PMNs were added to the apical chamber in the absence of fMLP. Data are expressed as pH (n = 3). (D) At T90, the difference between starting and ending pH were calculated. Data are expressed as change in pH. n

= number of independent experiments performed, separate passages of cells were used for each experiment. The data for each experiment were pooled and expressed as the mean ± SEM and p value determined by ANOVA. *$p < 0.05$, **$p < 0.01$, ****$p < 0.0001$

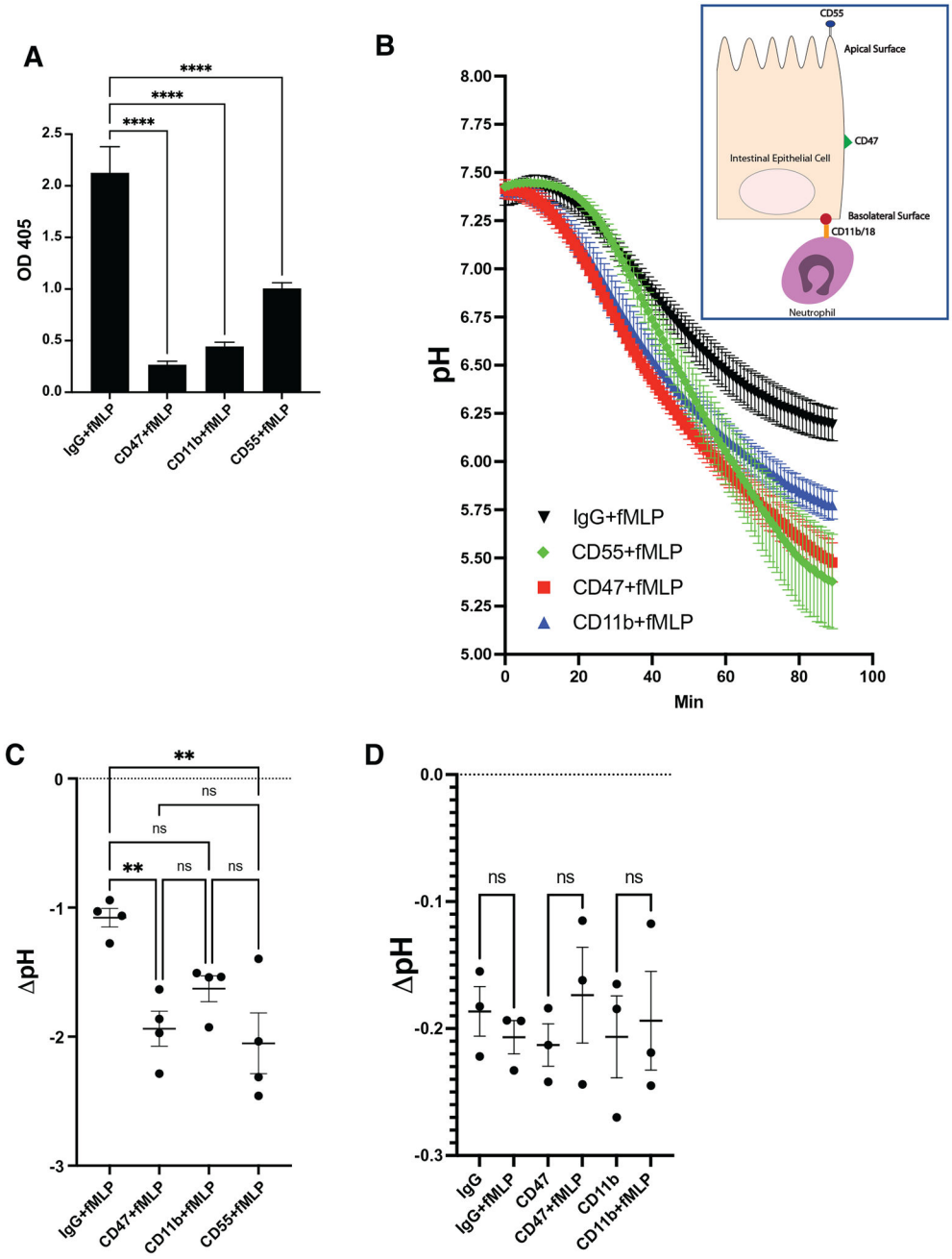

FIGURE 4.

Role of PMN TEM in extracellular acidification. (A) Quantification of MPO activity at T90 ($n = 4$). (B) Changes in extracellular pH. 1.5×10^6 PMNs were transmigrated basolateral to apical across confluent T84 monolayers in the presence or absence of 10 μg/ml anti-CD47, anti-CD11b, anti-CD55, or IgG controls and the extracellular pH was recorded every minute for 90 min. (C) At T90, the difference between starting and ending pH were calculated. Data are expressed as change in pH. Rat and mouse IgG controls were pool in the IgG+fMLP group. Data are expressed as pH ($n = 4$). (D) Changes in extracellular pH. 1.5×10^6 PMNs were transmigrated apical to basolateral across confluent T84 monolayers plated as inserts

in the presence or absence of 10 μg/ml anti-CD47, anti-CD11b, anti-CD55, or IgG controls and the extracellular pH was recorded every minute for 90 min. n = number of independent experiments performed, separate passages of cells were used for each experiment. The data for each experiment were pooled and expressed as the mean ± SEM and p value determined by ANOVA. ***$p < 0.001$, ****$p < 0.0001$

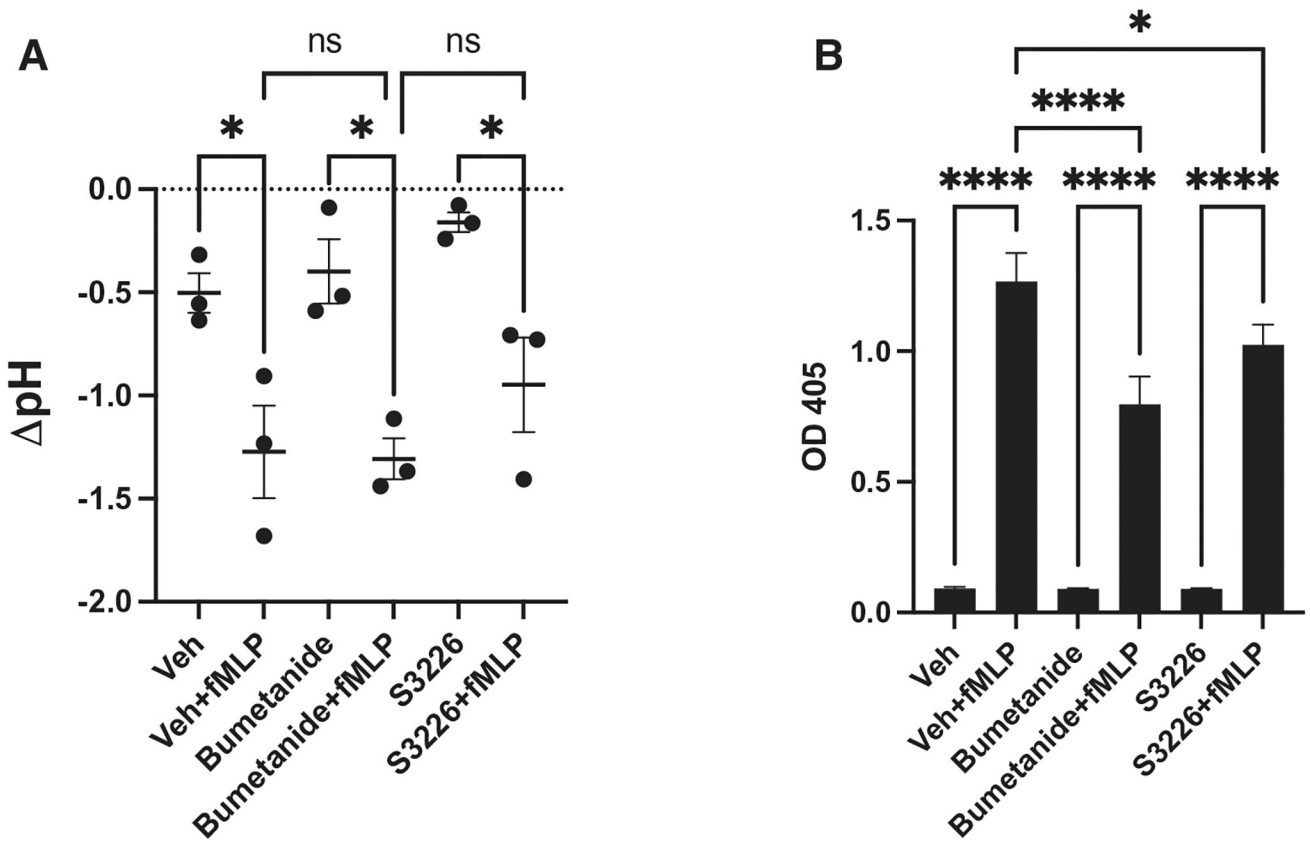

FIGURE 5.

Influence of ion transport on inflammatory acidification. (A) Change in extracellular acidification. 1.5×10^6 PMNs were transmigrated apical to basolateral across confluent T84 monolayers in the presence or absence bumetanide (10 μM) or S3226 (5 μM) for 90 min and the change in extracellular pH calculated. In the controls (Veh, Bumetanide, S3226), 1.5×10^6 PMNs were added to the apical chamber in the absence of fMLP. Data are expressed as change in pH. Data are expressed as pH ($n = 3$). (B) Quantification of MPO activity at T90 ($n = 3$). n = number of independent experiments performed, separate passages of cells were used for each experiment. The data for each experiment were pooled and expressed as the mean ± SEM and p value determined by ANOVA. *$p < 0.05$, ****$p < 0.0001$

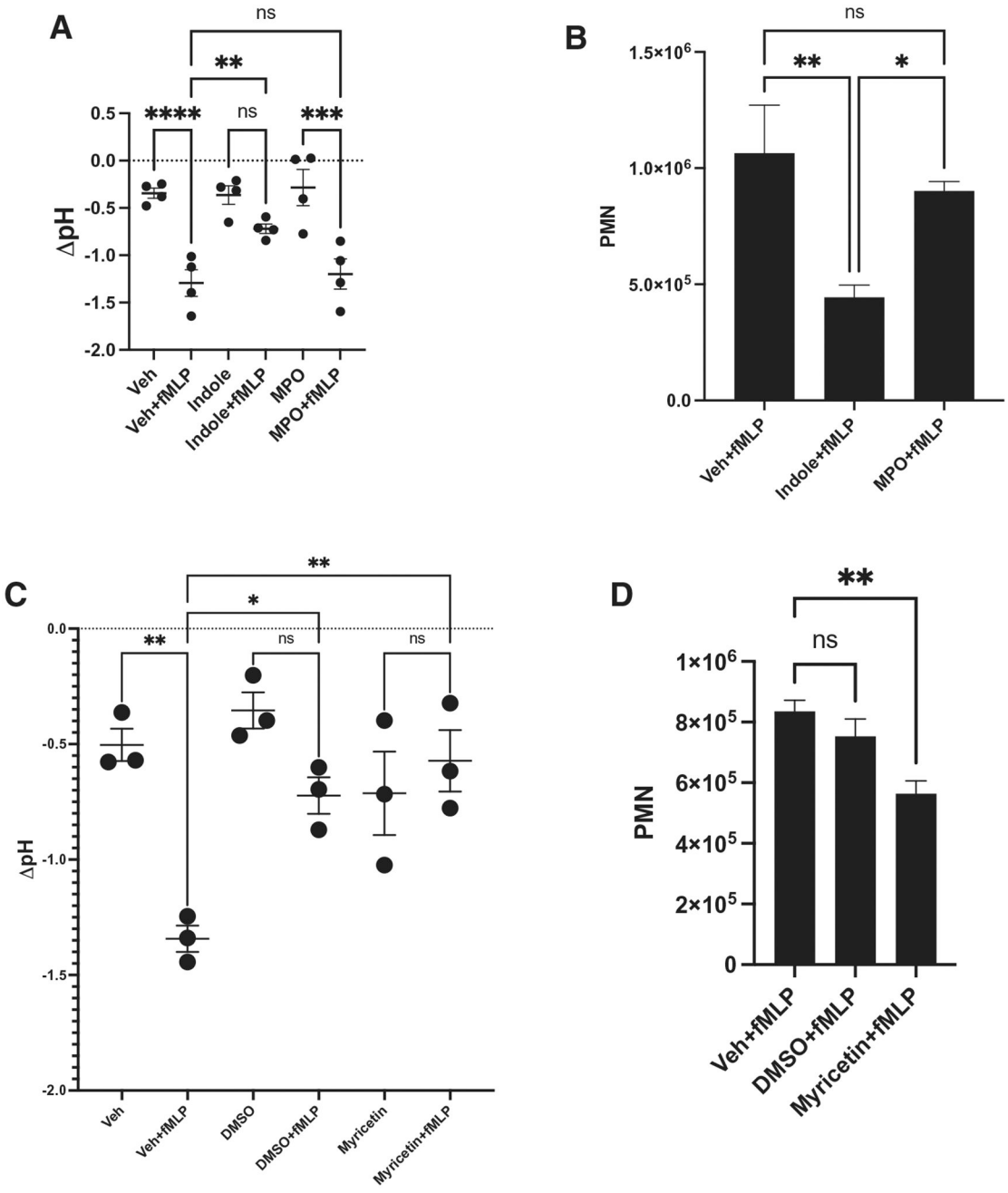

FIGURE 6.

Inflammatory acidification is independent of MPO. (A) Change in extracellular acidification. 1.5×10^6 PMNs were transmigrated apical to basolateral across confluent T84 monolayers in the presence or absence indole (1 mM) or 4-ABAH (500 μM) for 90 min and the change in extracellular pH calculated. In the controls, 1.5×10^6 PMNs were added in the absence of fMLP. Data are expressed as change in pH. Data are expressed as pH (n = 4). (B) Quantification of transmigrated PMN at T90 (n = 4). (C) Change in extracellular acidification. 1.5×10^6 PMNs were transmigrated basolateral to apical across confluent T84 monolayers in the presence or absence of 1% DMSO or 10 μM myricetin for 90 min and

the change in extracellular pH calculated. In the controls (Veh, DMSO, Myricetin), 1.5×10^6 PMNs were added to the apical chamber in the absence of fMLP. Data are expressed as change in pH. Data are expressed as pH ($n = 3$). (D) Quantification of transmigrated PMN at T90 ($n = 3$). n = number of independent experiments performed, separate passages of cells were used for each experiment. The data for each experiment were pooled and expressed as the mean ± SEM and p value determined by ANOVA. *$p < 0.05$, **$p < 0.01$, ***$p < 0.001$, ****$p < 0.0001$